Nuclear Quadrupole Interaction of ^{111}Cd as an Impurity in In, InBi, and In_2Bi in Relation to Ion Implantation

C. Budtz-Jørgensen, F. Abildskov, K. Bonde Nielsen, H. Ravn,* and U. Willumsen
Institute of Physics, University of Aarhus, DK-8000 Aarhus C, Denmark
(Received 30 May 1973)

The quadrupole interaction for ^{111}Cd (in the $5/2^+$ excited state) embedded in In, InBI, and In_2Bi is studied using the time-differential-perturbed-angular correlation technique. The interaction frequencies $\omega_0 = (3/20)e^2qQ\hbar^{-1}$ found for ^{111}Cd at substitutional lattice sites in these metals are ω_0(In) $= 16.8 \times 10^6$ rad/sec, ω_0(InBi, In site) $= 10.4 \times 10^6$ rad/sec, ω_0(In_2Bi, In_I site) $= 9.7 \times 10^6$ rad/sec, ω_0(In_2Bi, In_{II} site) $= 35.6 \times 10^6$ rad/sec, and ω_0(In_2Bi, Bi site) $= 29.6 \times 10^6$ rad/sec. Local contributions to the field gradients are found to be present, implying that the previous evaluations of $Q(^{111}Cd)$ should be attended to. For samples made by ion implantation of ^{111}In, it is found that $> 96\%$, $\approx 80\%$, and $\approx 84\%$ of the implanted atoms are substitutional at room temperature for In, InBi, and In_2Bi, respectively. The latter value includes $\approx 18\%$ of ^{111}In at the Bi site while, for InBi, all the substitutional atoms are at In sites.. The remaining implants are trapped in domains of radiation damage, characterized by a frequency distribution with a large average value $\bar{\omega}_0$ (for InBi $\bar{\omega}_0 \approx 45 \times 10^7$ rad/sec).

I. INTRODUCTION

Hyperfine interactions of dilute concentrations of impurity atoms in solids have been given much attention in recent years.[1,2] The increased interest in the subject originates to a great extent from the attempts of nuclear physicists to apply internal fields of atoms in solids for the determination of magnetic-dipole and electric-quadrupole moments of nuclear excited states. Since one is often concerned with in-beam experiments whereby an ion is recoiled into a target material, a number of problems related to the creation and annealing of radiation damage and to diffusion and location of the implanted atom (usually an impurity) immediately occur. Radioactivity studies of samples prepared by implantation of the probe activity by means of an isotope separator[3] supplement in-beam experiments and involve similar problems. The present paper deals with time-differential-perturbed-angular-correlation (TDPAC) studies of the hfs quadrupole interaction of ^{111}Cd impurity atoms in a number of metallic environments.[4] Samples of In, InBi, and In_2Bi were prepared either by ion implantation of the radioactive probe ^{111}In into these materials or chemically by adding the ^{111}In activity before producing the samples.

One purpose of the study is to compare the TDPAC patterns of the implanted samples with the corresponding data for the chemical samples. In the latter, the probe ^{111}Cd is expected to be located at regular In lattice sites, since the recoil energy in the electron-capture decay of ^{111}In is very small. Data of this kind can be valuable for the study of the defect solid state on the microscopic level as far as radiation damage, annealing, and impurity location are concerned. As to nuclear applications, it is important to learn more about conditions yielding well-defined target-impurity configurations and, for calibration purposes, to obtain the internal field gradients (internal magnetic fields) of different chemical elements embedded in various solid materials.

There exist NMR data on field gradients for bulk In[5] and InBi,[6] while a search for the quadrupole frequency in In_2Bi failed.[6] A point in choosing materials also being studied by the NMR or nuclear-quadrupole-resonance (NQR) techniques is the possibility of comparing the field gradients at impurity nuclei (in our case ^{111}Cd) with those at the nuclei of the bulk material (in our case ^{115}In). Experimental data on field gradients of dilute impurities in metals are scarce,[7] and reasons for attempting calculations have been weak, in view of the complexity already occurring in the understanding of the sources of quadrupole fields in the bulk materials.[8] However, a sufficient amount of systematic data of the kind presented in this paper may be helpful for the evaluation of the contribution of local field gradients to the total quadrupole frequency since, to a first approximation, the difference in field gradients between the bulk and the impurity case may be associated with their local contributions.

The data presented in Sec. III are discussed (Sec. IV) partly from the point of view of the implantation properties and partly from that of a comparison of the quadrupole frequencies.

II. EXPERIMENTAL TECHNIQUE

The reason for choosing ^{111}In as a radioactive probe (and hence also intermetallic compounds of indium as source materials) is primarily that the measurements are fairly simple to perform and also that sufficient statistical accuracy is obtained with a 3-day data accumulation for any given sample. The electron-capture decay $^{111}\text{In} \rightarrow {}^{111}$Cd pro-

ceeds (with a branching of >99%) through the $\frac{5}{2}^+$ 247-keV isomeric state of ^{111}Cd with $T_{1/2} \approx 84$ nsec via the 173–247-keV γ cascade. This cascade has a well-known angular correlation[9] with $A_{22} \approx -0.18$ and $A_{44} \approx 0$.

A. Source Preparation

The isotope ^{111}In was produced in a cyclotron via the reaction ^{109}Ag(α, $2n$) ^{111}In. After the addition of the In carrier and suitable chemical treatment, the ^{111}In activity ($T_{1/2} = 2.81$ day) was electroplated onto Cu foils or In foils with the purpose of fabricating ion-implanted or chemical samples, respectively.

While the InBi compound was made by melting indium (with or without tracer activity) with bismuth in the proper stoichiometric ratio, it is more difficult to make samples with the pure In_2Bi phase, as can be understood from the phase diagram of the In-Bi intermetallic compound.[10] In this case, zone melting was applied to make crystallites of In_2Bi which, in turn, were identified[11] via x-ray diffraction. For the ion-implantation studies, polycrystalline foils of In, InBi, and In_2Bi were rolled out and mechanically polished; the corresponding chemical samples were made into cylindrical bricks of the same materials with the ^{111}In activity added to yield source strengths of ≈ 10 μCi.

The implantation was performed by isotope separation of In from the electroplated Cu foils placed in the oven of the separator ion source. Since the stable indium isotopes are ^{113}In(4.3%) and ^{115}In(95.7%), separation of ^{111}In is very clean and sources of ≈ 10 μCi on a 2×5 mm spot, corresponding to a dose of $\approx 10^{12}$ atom/cm^2, could be collected without significant contamination of other isotopes. The implantation energy was ≈ 60 keV, corresponding to an average implantation depth[12] of ≈ 170 Å and a straggling of ≈ 85 Å. The dose was therefore one implanted atom per $\approx 10^4$ crystal atoms in the peak of the range distribution, and $\approx 95\%$ of the implants is screened from the surface by $\gtrsim 10$ atomic layers for all three samples.

B. Instrumentation

Since TDPAC measurements are a standard technique, only a few remarks on the experimental procedure will be appropriate. The hfs interaction of ^{111}Cd impurities at substitutional lattice sites is expected to be a pure static quadrupole with well-defined frequencies characterizing each particular type of site. Thus the functional form of the attenuation factor $G_2(t)$ for the chemical samples [see Sec. III, Eq. (1)] is known. Unlike this, the attenuation in the implanted samples will depend upon the number of In atoms which end up substitutional relative to the number of In atoms going into sites associated with crystal imperfections created as a result of the implantation process. The form of $G_2(t)$ is therefore unknown, and data must always be recorded at two different angles between the two γ counters in order to extract $G_2(t)$ from the spectrum. Below we shall briefly account for the precautions taken to meet the requirements to experimental stability.

1. Routing

The γ detectors used were 1.5 in. diam by 1 in. NaI(Tl) crystals, and the fast pulses provided a time resolution of 2.1 nsec at γ energies of ≈ 250 and ≈ 175 keV, respectively. Due to absorbers in front of the detectors eliminating the x rays, no prompt contribution to the time spectra generated by the time-to-amplitude converter (TAC) was present. By means of suitable delays a time spectrum, which is symmetric around $t = 0$, was placed in the middle of the TAC range (2 μsec). In order to eliminate the overlap between its two mirror parts, these were routed to different memory groups of the multichannel analyzer (MCA). This gave an immediate visual check of drift in the time branch of the apparatus, because the two mirror images are affected differently by drift—and rather drastically so—around $t \approx 0$. It also improved the subtraction of random coincidences which, in both routed spectra, appear cleanly as a constant level in front of the exponential part. Accurate random subtraction is crucial when the half-life of the perturbed state is smaller than the perturbation period.

2. Digital Stabilization

In order to completely avoid time shifts during the long counting period necessary, and in particular to avoid shifts between runs at different angles, the time spectrum was digitally stabilized. This was done in the analog-to-digital converter (ADC) by requiring that the difference between the number of counts in corresponding sets of channels on the two slopes of the "exponential" peak formed by the two mirror parts of the time spectrum be zero. In this way, the drift of the $t = 0$ position of the ADC was kept below 0.4 nsec. Digital stabilization was also applied on the energy branch of the system.

3. Normalization

Data were recorded at angles π and $\frac{1}{2}\pi$ between the two γ counters over ≈ 24-h periods and then normalized by means of the total number of single counts from the 247-keV transition recorded in the movable counter. Due to the decay of the source, the normalization will be affected by the dead time of the system. This is dealt with by recording the coincidence between the busy signal from the TAC and the (start-side) single channel (SCA), which

accepts the 247-keV pulses. The coincidences provide the proper normalization when small corrections for the dead time in the (stop-side) SCA and in the MCA are included. The normalization also takes care of small maladjustments of the centering of the sources with respect to the detectors. For the chemical samples self-absorption will affect the results, since here the difference for the coincident events and the single events has the same effect as if the distance between the movable counter and the source were larger in the π position than in the $\frac{1}{2}\pi$ position. The correction for self-absorption was calculated by means of the program developed by Lopiparo and Rasera, [13] and amounts to a decrease of $\approx 2\%$ in the measured anisotropy of the correlation.

III. RESULTS

For a polycrystalline sample (i.e., random distribution of the symmetry axis of the interaction), the expression for a directional angular correlation between radiations (1) and (2), influenced by extra nuclear perturbations, takes the form [with $A_{kk} \equiv A_k(1)A_k(2)$][14]

$$W(\theta, t) = 1 + \sum_{\substack{k=2, \\ \text{even } k}}^{k_{max}} A_{kk} G_k(t) P_k(\cos\theta) . \quad (1)$$

The correlation coefficients $A_k(1)$ and $A_k(2)$ are determined by the spins of the nuclear states and the multipolarities of the radiations. In the present case, $A_4(1) \approx 0$ and $k_{max} = 4$. The attenuation factors $G_k(t)$ result from coupling between the static nuclear moments and extra nuclear fields. It follows that in our case only $G_2(t)$ enters. For a pure static interaction of the nuclear quadrupole moment eQ with the electric-field gradient eq at the nucleus, and for the particular intermediate nuclear spin $I = \frac{5}{2}$, which is the one relevant here, the attenuation factor is given by

$$G_2(t) = \tfrac{1}{5} + \tfrac{13}{35}\cos(\omega_0 t) + \tfrac{2}{7}\cos(2\omega_0 t) + \tfrac{1}{7}\cos(3\omega_0 t) , \quad (2)$$

where $\omega_0 = \frac{3}{20} e^2 q Q \hbar^{-1}$.

If the samples are not perfectly polycrystalline, one may still formally apply Eq. (1) with

$$G_2(t) = \sum_{n=0}^{3} a_2^n \cos(n\omega_0 t) ; \quad (3)$$

in this case, however, the coefficients a_2^n will depend upon the orientations of the microcrystals with respect to the positions of the two counters and upon the ratio $A_4(2)/A_2(2)$. The polycrystalline relation

$$A_2(1)A_2(2)G_2^{exp}(t) = \frac{(1/Q_2)[N(\pi, t) - N(\frac{1}{2}\pi, t)]}{[\frac{1}{2}N(\pi, t) + N(\frac{1}{2}\pi, t)]} , \quad (4)$$

where Q_2 is the correction factor for finite solid angle and $N(\theta, t)$ the true coincidence-count rate, is not valid either, although it may still be a useful approximation when the sample is not far from being an ideal polycrystal.

Data from representative runs are displayed in Fig. 1. The left- and right-hand columns show $G_2^{exp}(t)$ for the chemical and the implanted samples, respectively. The solid curves are least-squares fits, obtained under the option that $G_2^{exp}(t)$ may reflect more than one site for the ^{111}Cd impurity atom and therefore can be a superposition of attenuation factors of the form given in Eq. (2) [or Eq. (3) with free parameters a_2^n].

In the analysis of the implantation data, it was assumed that $G_2^{exp}(t)$ has the form given by Eq. (2) superimposed on a constant term, and (implicitly) that there is a steep decrease of $G_2^{exp}(t)$ in the first few channels of the spectra. These channels are omitted in the analysis. Table I is a presentation of the frequencies ω_0 obtained from the least-squares fit, together with f, the weight factor associated with each $G_2(t, \omega_0)$, using $A_{22} = -0.176$.

For the In metal the a_2^n's of the chemical samples always corresponded to values of a polycrystalline

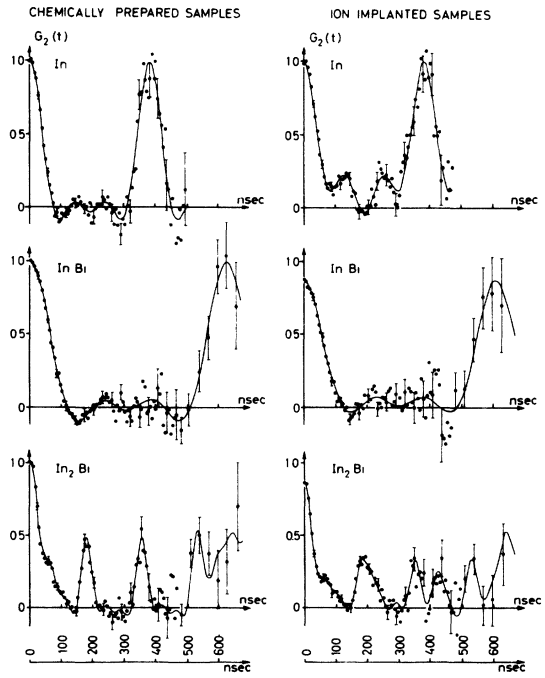

FIG. 1. Experimental attenuation factors $G_2^{exp}(t)$ (representative data). The solid curves are computer fits performed as described in the text. Using $G_2^{exp}(t = 0) \equiv 1$, the fits to the chemical samples yield $A_{22} = -0.176 \pm 0.002$, which is used throughout for normalization. Our value for A_{22} is slightly smaller than that usually quoted (Ref. 9). The difference may be related to the effect of self-absorption in the sources. Without correction for self-absorption, our value becomes -0.180 ± 0.002, in perfect agreement with Ref. 9.

TABLE I. Summary of quadrupole frequencies $\omega_0 = \frac{3}{20} e^2 qQ\hbar^{-1}$ for substitutional ^{111}Cd in In, InBi, and In_2Bi. The quantity f measures the relative amount of ^{111}In activity associated with each ω_0 (i.e., the activity associated with each lattice site). The quoted values are averages for several runs of the kind displayed in Fig. 1. The errors given reflect the reproducibility of the individual runs.

	Lattice Atoms		Ion-Implanted Atoms	
Host	ω_0 (10^6 rad/sec)	f	ω_0 (10^6 rad/sec)	f
In	16.8[a] ± 0.1	1.00 ± 0.02	16.9 ± 0.1	0.98 ± 0.02
InBi	10.4[b] ± 0.1	1.00 ± 0.02	10.3 ± 0.2	0.80 ± 0.02
In_2Bi	9.7 ± 0.1	0.50 ± 0.02	9.9 ± 0.3	0.34 ± 0.02
	35.6[b] ± 0.1	0.50 ± 0.02	35.7 ± 0.1	0.32 ± 0.02
			29.6 ± 0.2	0.18 ± 0.02

[a]Agrees with earlier published values of Refs. 4 and 22.

[b]Agrees with recent values of Ref. 7. The presentation of In_2Bi data in this reference only indicates the high-frequency site. The small A_{22}^{eff} quoted in Ref. 7 is consistent with the f value given here.

material [see Eq. (2)], while, depending on the preparation of the target foils, the a_2^n's of the implanted samples reflected crystallographic texture[15] in the surface of the foil. This is clearly seen in the top right-hand side of Fig. 1, which shows data from a sample where the effect of texture turned out to be particularly large; one obtains [cf. comments to Eq. (3)] $a_2^0 : a_2^1 : a_2^2 : a_2^3$ = 0.33(1) : 0.33(1) : 0.18(1) : 0.16(1), compared to the polycrystalline values 0.20 : 0.37 : 0.29 : 0.14. (The foil used in this case was made by evaporation, while rolled foils showed less texture; this statement is based on the examination of a few foils only.) There is no evidence of a distribution of field gradients in either the chemical samples or in the implanted samples.

For the intermetallic compound InBi, the effect of texture was negligible. It appears that only about 80% of the implanted atoms show the same perturbation pattern as the chemical sample. In order to further examine this, we performed a measurement with an expanded time scale on the same sample. Figure 2 shows the data obtained when the function $fG_2(t, \omega_0)$ from the analysis mentioned above is subtracted from the raw data of the expanded run and the result multiplied by $(1-f)^{-1}$. Here the solid curve represents a least-squares fit to a Gaussian distribution of quadrupole frequencies, yielding $\bar{\omega}_0 \approx 45 \times 10^7$ rad/sec and $\sigma(\omega_0)/\bar{\omega}_0 \approx 50\%$. (Strictly speaking, an asymmetry parameter η should be included; however, it does not affect the order-of-magnitude estimate of $\bar{\omega}_0$.) The "hard core" of this fit corresponds to the constant term included in the fit of Fig. 1. For the regular site, there is no evidence of a distribution of frequencies around ω_0, but the analysis is rather insensitive to this because $2\pi\omega_0^{-1} \gg T_{1/2}$.

In the case of In_2Bi, the data for the chemical sample are fitted under the assumption of two quadrupole frequencies with equal-weight factors, since there are two unequal In sites per unit cell,[11] both with an axially symmetric field gradient. It is not possible to analyze the implanted samples under this assumption, even if one allows for frequency distributions and also includes a constant term similar to that in the InBi case. However, when just one extra frequency is included, an excellent fit with two of the frequencies identical to those of the chemical sample is obtained. Similar to the case for InBi, it is found that some (i.e., ≈16%) ^{111}In implants are at a "site" characterized by frequency distribution.

IV. COMMENTS

A. Implantation

The data presented in Sec. III may be summarized in the following way: For all three samples, large fractions (i.e., >96%, ≈80%, and ≈84% for In, InBi, and In_2Bi, respectively) end up substitutionally, as shown by the fact that the observed frequencies are identical to those of the chemical samples. Furthermore, the absence of a frequency distribution indicates that these sites are not associated with nearby imperfections in the crystal. Since the concentration of the damage created along the track of the impinging ion is very large,[16] one expects that the annealing at room temperature has played an important role. To obtain more information on the influence of annealing on the frequency patterns, low-temperature measurements or (due to the different time scale) in-beam experiments might be considered.

In the compounds InBi and In_2Bi, the existence of sites characterized by a frequency distribution with a very large average frequency (i.e., $\bar{\omega}_0 \approx 45 \times 10^7$ rad/sec) suggests that some of the implanted ^{111}In ions are trapped in a damage region (e.g., a

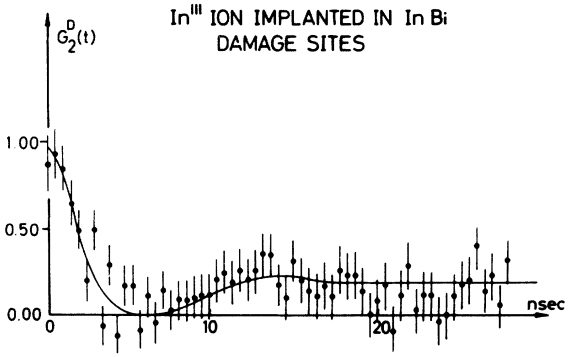

FIG. 2. Data for the implanted InBi sample (Fig. 1) recorded with expanded time scale. The experimental points are $[G_2^{exp}(t) - f G_2(t, \omega_0)](1-f)^{-1}$, where (as described in the text) f and ω_0 are obtained from the least-squares fit to the data of Fig. 1. The solid curve $G_2^D(t)$ is a computer fit (including the effect of finite time resolution) obtained under the assumption that the data can be represented by a Gaussian frequency distribution. The fit yields the parameters $\bar{\omega}_0 \approx 45\times10^7$ rad/sec and $\sigma(\omega_0)/\bar{\omega}_0 \approx 50\%$.

vacancy cluster). Considering the low implantation dose (i.e., track distance ≈ 100 Å) and dose rate ($\approx 5\times10^8$ ion/cm^2 sec), we interpret the quantity $1-\sum_i f_i$, where f_i is listed in Table I as being the probability that the impinging atom is trapped in domains of self-induced damage, which are stable during room-temperature annealing. Using the graphs of Ref. 17, one may estimate that the probability for an implanted ion to "thermalize" inside the region of initially created damage is $\gtrsim 50\%$ in our cases, which is consistent with the suggested interpretation of $1-\sum_i f_i$. The possibility that one is dealing with a surface effect is not likely since, again, there is no evidence of a frequency distribution for implantation in In metal, and the implantation range and straggling are similar for In, InBi, and In_2Bi (see Sec. II).

The present results may be compared with a recent TDPAC study[18] of the damage around ^{111}In implanted in silver via the $(\alpha, 2n)$ reaction. In this work it is reported that $\approx 3\%$ of the implants experience a large unique field gradient ($\omega_0 = 15.7 \times10^7$ rad/sec), which is suggested to be caused by a vacancy in one of the $\langle 100\rangle$ sites close to the implanted ion. Similarly, for InBi and In_2Bi, a missing neighbor (say, in the nearest Bi site) would produce a field gradient of $\approx 4\times10^{16}$ V/cm^2, which is one order of magnitude larger than the corresponding value for the lattice sites quoted in Table II. It is therefore likely that the origin of the observed distribution (Fig. 2) is defects very close to the implant. The fact that the frequency is not sharp suggests that more than one configuration of interstitial and/or vacancies are involved, pointing to a defect type different from that seen in Ag. A "longer-range" effect of point defects, like that indicated by the slow component of Ref. 18, is not observed either since, again, there is no significant frequency spread on the lattice sites in any of the samples studied. Also, we observed no changes in the fraction of implants at the lattice sites during a 6-day room-temperature annealing.

The third frequency ($\omega_0 = 29.6\times10^6$ rad/sec) found in In_2Bi is of the same order of magnitude as those of the regular In sites. The discussion above indicates that this frequency cannot be associated with a unique damage site such as a nearest-neighbor vacancy because that would produce too large a field gradient. Furthermore, the observed ω_0 corresponds rather well to the gradient at the Bi site estimated from the lattice contribution (see Table II). The results thus suggest that a certain fraction of ^{111}In goes into the Bi site in In_2Bi, while the Bi site in InBi is unstable with regard to a substitution of an In impurity by implantation. [It is not likely that the frequencies of the two sites in InBi are almost equal, since the lattice contribution to eq (see Sec. IV B) is about three times larger for the Bi site than for the In site.]

B. Quadrupole Frequency

It is customary to speak about electric-field gradients in metals in terms of a lattice contribution and a local contribution; hence one has[8]

$$eq = (1-R)eq_{loc} + (1-\gamma'_\infty)(1+\delta)eq_{lat}\,. \qquad (5)$$

Here the eq_{lat} is the classical field gradient calculated by superposition of the Coulomb fields from the lattice-point charges corresponding to the ionic cores of the metal atoms.[19] The term eq_{lat} may also include contributions from the atomic dipoles and quadrupoles which may be induced by the action of the crystal field itself.[20] The conduction electrons do not contribute to eq_{lat}, since they are treated as being uniformly distributed throughout the crystal. The factor $1+\delta$ then enters to correct this by introducing effective charges (which may differ for different atoms in the unit cell of a compound). The concept of effective charges reflects the fact that, to a certain extent, the conduction electrons are expelled from a region [the augmented-plane-wave (APW) sphere][8] around the crystal atoms. The Sternheimer factor $1-\gamma_\infty$ accounts for the field-gradient enhancement at the nucleus due to the polarization of the closed shells of the crystal atoms, which is caused by the crystal field. The closed shells are treated as free ions in the calculations of $1-\gamma_\infty$, and are thus independent of the lattice for a given atom. The prime in Eq. (5) indicates that this is not strictly so because of the modifications of the closed-shell wave functions when the ions are packed into a metal. The term eq_{loc} is the contribution to the

TABLE II. Quadrupole coupling constatns derived from the data in Table I. Data for the bulk materials and calculations of eq_{lat} are included.

Host	Lattice Site (coordinates)	$\lvert eqQ \rvert$ (10^{-8} V) ^{111}Cd	^{115}In	eq_{lat}[a] (10^{15} V/cm^2)	$\lvert eqQ/(1-\gamma_\infty)eq_{lat} \rvert$ (10^{-24} cm^2) ^{111}Cd[b]	^{115}In[c]
In	In $\begin{matrix}(\frac{1}{2}\ \frac{1}{2}\ \frac{1}{2})\\(0\ 0\ 0)\end{matrix}$	7.37	12.19[d]	−1.50	1.62	3.14
InBi	In $\begin{matrix}(0\ 0\ 0)\\(\frac{1}{2}\ \frac{1}{2}\ 0)\end{matrix}$	4.56	2.74[e]	2.95	0.51	0.31[f]
	In $\begin{matrix}(0\ 0\ 0)\\(0\ 0\ \frac{1}{2})\end{matrix}$	4.26		−1.09	1.29[g]	
In_2Bi	In $\begin{matrix}(\frac{1}{3}\ \frac{2}{3}\ \frac{1}{4})\\(\frac{2}{3}\ \frac{1}{3}\ \frac{3}{4})\end{matrix}$	15.61		−1.44	3.58[g]	
	Bi $\begin{matrix}(\frac{2}{3}\ \frac{1}{3}\ \frac{1}{4})\\(\frac{1}{3}\ \frac{2}{3}\ \frac{3}{4})\end{matrix}$	12.99		−2.16	1.98	

[a]The eq_{lat} are calculated according to the method developed by de Wette (Ref. 19), using the lattice constants (a, c) equal to (3.244 Å, 4.938 Å), (5.005 Å, 4.771 Å), and (5.496 Å, 6.579 Å) for tetragonal In, tetragonal InBi, and hexagonal In_2Bi, respectively.

[b]$\gamma_\infty(Cd) = -29.3$, Ref. 21.

[c]$\gamma_\infty(In) = -24.9$, Ref. 21.

[d]Reference 5.

[e]Reference 6.

[f]We have not been able to reproduce the value quoted for eq_{lat}(InBi) in Ref. 6.

[g]The assignment of the particular In sites to the measured frequencies ω_0 is tentative.

field gradients from the conduction electrons located in a suitably chosen cell around the particular crystal atom, in which the gradient is calculated. The factor $1-R$ accounts for the effect of polarization of the closed-shell electrons by eq_{loc}.

Table II summarizes the quadrupole-coupling constants obtained in the present work. It is instructive to compare the experimental data with calculated[19,21] values of $(1-\gamma_\infty)eq_{lat}$. The variation appearing in column 6 clearly demonstrates the need for either including the term $(1-R)eq_{loc}$ or the factor $1+\delta$, or both. Although δ may be very small, one must consider the possibility that in the compounds the effect of such a term may be enhanced. This may be so because the resulting field gradients appear as differences between large contributions $[(1+\delta^i)eq^i_{lat}]$ from the various sublattices involved in the summation and can thus be sensitive to even small readjustments of the charges assigned to each type of lattice site.

It is also interesting to compare with corresponding data for the bulk material (i.e., NMR or NQR measurements of eq for ^{115}In). Such data are available for In and InBi and are included in Table II. If the term $(1-R)eq_{loc}$ were negligible, the ratios between the figures given in columns 7 and 6 would be equal to $[1-\gamma_\infty(Cd)]Q(^{115}In)/[1-\gamma_\infty(In)]Q(^{111}Cd)$ and thus be independent of the host material. Since this is not the case, important local contributions to eq must be present in at least one (and presumably in all) of the four cases. This casts doubt upon a calculation by Bodenstedt *et al.*[22] of the nuclear quadrupole moment of ^{111}Cd [$Q(^{111}Cd) = 0.44$ b], which presumed that the term $(1-R)eq_{loc}$ can be neglected. This presumption is based upon the experimental observation that the temperature dependence of eq is very similar for ^{111}Cd and ^{115}In at the lattice sites of the In metal. The additional data on InBi given here are inconsistent with this interpretation unless there is a large local contribution in InBi but none in In, which seems to be unlikely. Furthermore, it appears that the term $1+\delta$, which has to be included for In in order to explain the observed values of the field gradients, in the absence of a local term, is rather large.

In a recent paper, Raghavan *et al.*[23] compared the quadrupole interaction in the $\frac{5}{2}^+$ and $\frac{3}{2}^+$ excited states of ^{111}Cd and ^{117}In, respectively. In a number of compounds (ionic salts of Cd), these authors found that $eq(^{111}Cd)$ and $eq(^{117}In)$ are broadly in proportion. From $Q(^{117}In) = 0.644$ b, using $eq(^{111}Cd)/[1-\gamma_\infty(Cd)] = eq(^{117}In)/[1-\gamma_\infty(In)]$, $Q(^{111}Cd) = 0.77$ b was yielded. The analysis of Raghavan *et al.* is convincing. However, the fact that, in at least one of the ionic compounds studied ($CdCl_2$),

the observed value of eq deviates rather a lot from the point-lattice value $[eq/(1-\gamma_\infty)eq_{\text{lat}} = 0.45]$ requires further attention before the evaluation of $Q(^{111}\text{Cd})$ can be considered final.

The problem involved in determining $Q(^{111}\text{Cd})$ may serve as an illustration of the way in which systematic information on field gradients of similar probes in various compounds can help establish the origin of the field gradients and be useful for the evaluation of nuclear quadrupole moments. It also calls for further theoretical work.

ACKNOWLEDGMENTS

It is a pleasure to acknowledge the cooperation of the cyclotron staff at The Niels Bohr Institute, Copenhagen, who produced the ^{111}In activity, the isotope-separator staff at the Institute of Physics, Aarhus, who performed the implantations, and the Department of Inorganic Chemistry at the Institute of Chemistry, Aarhus, which placed the zone-melting apparatus and an x-ray precession camera at our disposal.

*Present address: CERN, CH-1211 Geneva 23, Switzerland.

[1] *Hyperfine Structure and Nuclear Radiations*, edited by E. Matthias and D. Shirley (North-Holland, Amsterdam, 1968).

[2] *Hyperfine Interactions in Excited Nuclei*, edited by G. Goldring and R. Kalish (Gordon and Breach, New York, 1971).

[3] H. de Waard and S. A. Drentje, Phys. Lett. **20,** 38 (1966); B. I. Deutch, P. Hornshøj, K. Bonde Nielsen, and F. Boehm, Phys. Lett. **21,** 659 (1966).

[4] P. Lehmann and J. Miller, J. Phys. Radium **17,** 526 (1956).

[5] W. T. Anderson, Jr., F. C. Thatcher, and R. R. Hewitt, Phys. Rev. **171,** 541 (1968); W. W. Simmons and C. P. Slichter, Phys. Rev. **121,** 1580 (1961).

[6] D. L. Radhakrishna Setty and B. D. Mungurwadi, Phys. Rev. **183,** 382 (1969); D. L. Radhakrishna Setty and B. D. Mungurwadi, Proc. Phys. Soc. Lond. **90,** 495 (1969).

[7] During the writing of the present paper, a comprehensive TDPAC study of quadrupole interactions in a variety of compounds has been published [H. Haas and D. A. Shirley, J. Chem. Phys. **58,** 3339 (1973)].

[8] R. E. Watson, A. C. Gossard, and Y. Yafet, Phys. Rev. **140,** A375 (1965); N. C. Mohapatra, C. M. Singal, and T. P. Das, Phys. Rev. Lett. **29,** 456 (1972); K. C. Das and R. K. Ray, Phys. Rev. **187,** 777 (1969); Solid State Commun. 8, 2025 (1970); J. Pelzl, Z. Phys. **251,** 13 (1972).

[9] R. M. Steffen, Phys. Rev. **103,** 116 (1956).

[10] M. Hansen, *Constitution of Binary Alloys*, 2nd ed. (McGraw-Hill, New York, 1958).

[11] E. S. Makarov, Kristallografiya 3, 5 (1958) [Sov. Phys.-Crystallogr. **3,** 3 (1958)].

[12] H. E. Schiøtt, Radiat. Eff. **6,** 107 (1970).

[13] D. C. Lopiparo and R. L. Rasera, in *Angular Correlations in Nuclear Disintegration*, edited by H. van Krugten and B. van Nooijen (Wolters-Noordhoff, Groningen, 1971), p. 66.

[14] H. Frauenfelder and R. M. Steffen, in *Alpha-, Beta-, and Gamma-Ray Spectroscopy*, edited by K. Siegbahn (North-Holland, Amsterdam, 1965), Chap. 19.

[15] E. N. Kaufman, Nucl. Instrum. Methods **103,** 447 (1972).

[16] G. H. Kinchin and R. S. Pease, Rep. Prog. Phys. **18,** 1 (1955); K. B. Winterbon, P. Sigmund, and J. B. Sanders, K. Dan. Vidensk. Selsk. Mat.-Fys. Medd. 37, No. 14 (1970).

[17] J. E. Westmoreland and P. Sigmund, Radiat. Eff. **6,** 187 (1970).

[18] M. Behar and R. M. Steffen, Phys. Rev. C **7,** 788 (1973).

[19] F. W. de Wette, Phys. Rev. **123,** 103 (1961).

[20] T. T. Taylor, Phys. Rev. **127,** 120 (1962).

[21] F. D. Feiock and W. R. Johnson, Phys. Rev. **187,** 39 (1969).

[22] E. Bodenstedt, W. H. Ellis, and U. Ortabasi, Phys. Rev. B **6,** 2909 (1972).

[23] R. S. Raghavan, P. Raghavan, and J. M. Friedt, Phys. Rev. Lett. **30,** 10 (1972).